J|A|C|S
ARTICLES
Published on Web 04/21/2007

Ab initio Study of the Excited-State Deactivation Pathways of Protonated Tryptophan and Tyrosine

Gilles Grégoire,*,† Christophe Jouvet,‡ Claude Dedonder,‡ and Andrzej L. Sobolewski§

Contribution from the Laboratoire de Physique des Lasers du CNRS, Institut Galilée, Université Paris 13, 93430 Villetaneuse, France, Laboratoire de Photophysique Moléculaire du CNRS, Bât. 210, Université Paris-Sud, F-91405 Orsay, France, and Institute of Physics, Polish Academy of Sciences, PL-02668 Warsaw, Poland

Received December 18, 2006; E-mail: gregoire@lpl.univ-paris13.fr

Abstract: In recent experiments, the excited-state lifetimes of protonated aromatic amino acids ($TrpH^+$ and $TyrH^+$) have been recorded by means of pump−probe photodissociation technique. The lifetime of $TyrH^+$ is much longer than that of $TrpH^+$, which has been initially rationalized on the basis of a simple phenomenological model. Besides, specific photofragments including the formation of radical cation after hydrogen loss are observed for $TrpH^+$ that are not found for $TyrH^+$. The *ab initio* calculations reported here for $TrpH^+$ and $TyrH^+$ using a coupled-cluster method are meant to track the rich photochemistry of these protonated amino acids following UV excitation.

Introduction

Among naturally occurring amino acids, three possess fluorescent aromatic chromophores: tryptophan (Trp), tyrosine (Tyr), and phenylalanine (Phe). Among them, Trp has been the most studied owing to its strong fluorescence yield and the rich variety of information it provides according to the possible environments.[1] By monitoring the Trp fluorescence in proteins, one can noninvasively diagnose malignancy in cells.[2,3] To understand the mechanism of fluorescence spectroscopy for cancer detection and to further improve its efficiency,[4] the understanding of the primary photoprocesses occurring in the bare molecule is nevertheless required. Interestingly, Trp fluorescence lifetime and intensity vary by orders of magnitude when the pH varies and drops dramatically at low pH when Trp is fully protonated, emphasizing a predominant nonradiative process.[1] H. Shizuka et al. have shown that the fluorescence intensity increases significantly when Trp complexes with 18-crown-6.[5] This observation suggests that the ammonium group plays a key role in the internal quenching of Trp. It has been stated that internal quenching is caused by electrophilic protonation by the ammonium ion at a different carbon position of the excited indole ring[6,7] according to the rotamer model.[8,9] In proteins, depending on local structural assembly, the excited-state could be quenched by neighboring peptide bonds and other amino acid residues.[10] This quenching is thought to mainly occur via through-space charge-transfer reactions such as with a disulfide bond (cystine), tyrosine, or positively charged histidine.[11] From these extensive experimental studies, it thus seems that electron transfer and/or proton-transfer processes play a key role in the excited-state properties of Trp. With the help of high level *ab initio* calculations that can be performed nowadays, one should be able to tackle this fundamental question.

Although the fluorescence of Trp has been widely studied experimentally as reported above, only few *ab initio* calculations have been undertaken on the excited-state properties of aromatic amino acids. M. A. Robb et al. recently report computational study on the fluorescence quenching of zwitterionic tryptophan at the CASSCF/6-31G* level.[12] Hydrogen transfer process in the excited-state from the protonated amino group to the indole chromophore has been proposed to rationalize the fluorescence quenching of tryptophan at neutral and slightly acidic pH. This hydrogen transfer goes through a conical intersection where the reaction path bifurcates toward either a completed hydrogen

† Université Paris 13.
‡ Université Paris-Sud.
§ Polish Academy of Sciences.

(1) Lakowicz, J. R. *Principles of Fluorescence Spectroscopy*, 2nd ed.; Kluwer Academic/Plenum: New York, 1999.
(2) Palmer, G. M.; Keely, P. J.; Breslin, T. M.; Ramanujam, N. *Photochem. Photobiol.* **2003**, *78*, 462−469.
(3) Grossman, N.; Ilovitz, E.; Chaims, O.; Salman, A.; Jagannathan, R.; Mark, S.; Cohen, B.; Gopas, J.; Mordechai, S. *J. Biochem. Biophys. Methods* **2001**, *50*, 53−63.
(4) Anidjar, M.; Ettori, D.; Cussenot, O.; Meria, P.; Desgrandchamps, F.; Cortesse, A.; Teillac, P.; Duc, A. L.; Avrillier, S. *J. Urology* **1996**, *156*, 1590.
(5) Shizuka, H.; Serizawa, M.; Shimo, T.; Saito, I.; Matsuura, T. *J. Am. Chem. Soc.* **1988**, *110*, 1930−1934.
(6) Yu, H. T.; Colucci, W. J.; McLaughlin, M. L.; Barkley, M. D. *J. Am. Chem. Soc.* **1992**, *114*, 8449−8454.
(7) Eftink, M. R.; Jia, Y. W.; Hu, D.; Ghiron, C. A. *J. Phys. Chem.* **1995**, *99*, 5713−5723.
(8) Robbins, R. J.; Fleming, G. R.; Beddard, G. S.; Robinson, G. W.; Thistlethwaite, P. J.; Woolfe, G. J. *J. Am. Chem. Soc.* **1980**, *102*, 6271−6279.
(9) Ruggiero, A. J.; Todd, D. C.; Fleming, G. R. *J. Am. Chem. Soc.* **1990**, *112*, 1003−1014.
(10) Adams, P. D.; Chen, Y.; Ma, K.; Zagorski, M. G.; Sonnichsen, F. D.; McLaughlin, M. L.; Barkley, M. D. *J. Am. Chem. Soc.* **2002**, *124*, 9278−9286.
(11) Chen, Y.; Barkley, M. D. *Biochemistry* **1998**, *37*, 9976−9982.
(12) Blancafort, L.; Gonzalez, D.; Olivucci, M.; Robb, M. A. *J. Am. Chem. Soc.* **2002**, *124*, 6398−6406.

transfer leading to a ground state tautomer or a decarboxylation product tryptamine. An alternative mechanism has also been proposed by P. R. Callis et al., where the quenching of the $\pi\pi^*$ state is due to charge transfer to the C═O peptide backbone.[13−15]

In the case of neutral aromatic molecules such as phenol and indole (the chromophores of Tyr and Trp, respectively),[16−19] it has been shown that nonradiative decays involving couplings with dissociative excited states play a key role in the photophysical properties of these molecules. Beside the two well-known electronic states of indole, L_a and L_b of $\pi\pi^*$ nature, recent quantum calculations have invoked a nearby $\pi\sigma^*$ excited state, dissociative along the indole N−H stretch coordinate.[20] However, because of the lack of experimental data, only very sparse theoretical works have been devoted to the excited-state properties of protonated Trp. Nevertheless, all of these studies have pointed out the presence of a low-lying $\pi\sigma^*$ excited-state independently of the method used, either TD−DFT,[21,22] DFT/MRCI,[23] or CC2.[24] In the particular case of TD−DFT calculations, a low-lying charge-transfer state where the electron is mainly localized on the acidic group is predicted. However, this is an artifact of the TD−DFT method that tends to underestimate the CT state[25] energy and as evidenced by the other calculations at the MRCI and CC2 level.

UV photoexcitation studies of gas-phase protonated amino acids molecules have emerged in recent years with the combination of mass spectrometry and laser spectroscopy techniques. Several experimental groups have investigated in both frequency and time domains the fragmentation of these biomolecules after UV absorption (UV-LID).[23,26−29] Comparison with conventional collision induced dissociation (CID) experiments has revealed that among the ionic fragmentation channels observed, some are common to both excitation schemes whereas a new de-activation pathway, namely formation of radical species following H atom loss, is evidenced in the UV-LID fragmentation pattern. If the former ones can be assigned to internal conversion process to the electronic ground state, the latter seems to imply a direct dissociation in the excited-state prior to energy redistribution (IVR) that leads to nonstatistical type of fragmentation.[30] Furthermore, small peptides containing aromatic amino acids also exhibit a rich photo fragmentation pattern, with the presence or not of radical species.[31] Interestingly, even when the aromatic residue is not directly protonated but embedded in GWG or GYG tripeptide, a rather short lifetime has been recorded that emphasizes a through-space mechanism for the electron transfer from the locally excited $\pi\pi^*$ state to the $\pi\sigma^*$ state located on the protonated amino group of the N-terminal glycine.[32]

In the view of these recent experimental data, we have already undertaken an *ab initio* study using the coupled-cluster method with single and double excitation (CC2) of the excited-state properties of protonated tryptamine that exhibits a simpler fragmentation pattern with the presence of both radical and internal conversion type fragments. Excited-state structure optimization has been performed and has revealed the very important role of an excited-state dissociative along the NH stretch of the protonated amino group, the $\pi\sigma^*$ state.[24] The coupling between the optically excited $\pi\pi^*$ state and the $\pi\sigma^*$ state induces an electron transfer from the indole ring toward the NH_3^+ group, which results in the neutralization of the amino group producing an unstable radical species, as for NH_4. H atom loss reaction occurs through a small barrier of 0.1 eV. In the course of the reaction, the $\pi\sigma^*$ state crosses the electronic ground state potential surface with the possibility of H recombination and internal conversion process.

Applying this model and using simple energetic to aromatic amino acids, namely tryptophan and tyrosine, we could predict that the excited $\pi\sigma^*$ state should be in the vicinity of the locally excited $\pi\pi^*$ state, with an energy gap larger in tyrosine than in tryptophan.[27] The aim of this study is to give an exhaustive and comprehensive picture of the excited-state properties of these two amino acids using high level *ab initio* methods. Enlightened, the intrinsic properties of these simple molecules may provide a good starting point for further investigations on larger peptides. We have calculated vertical excitation energies for several low-lying isomers of protonated tyrosine and tryptophan and performed geometry optimizations of the first excited states to explore the possible deactivation pathways involved in these protonated species.

Computational Methods

Not all conformers of the systems that could be present in the experiments are considered in the present work. The most relevant structures that are essential for explanation of the photoinduced processes have been selected with a molecular-mechanics search. The ground-state geometry of the most stable structures preselected in this way was next optimized with the second-order Møller-Plesset (MP2) method.

Excitation energies and response properties have been calculated with the CC2 method,[33] which is a simplified and cost-effective variant of the coupled-cluster method with single and double excitations. CC2 can be considered as the equivalent of MP2 for excited electronic states.

(13) Vivian, J. T.; Callis, P. R. *Biophys. J.* **2001**, *80*, 2093−2109.
(14) Callis, P. R.; Vivian, J. T. *Chem. Phys. Lett.* **2003**, *369*, 409−414.
(15) Callis, P. R.; Liu, T. Q. *J. Phys. Chem. B* **2004**, *108*, 4248−4259.
(16) Pino, G.; Gregoire, G.; Dedonder-Lardeux, C.; Jouvet, C.; Martrenchard, S.; Solgadi, D. *Phys. Chem. Chem. Phys.* **2000**, *2*, 893−900.
(17) Gregoire, G.; Dedonder-Lardeux, C.; Jouvet, C.; Martrenchard, S.; Solgadi, D. *J. Phys. Chem. A* **2001**, *105*, 5971−5976.
(18) Ashfold, M. N. R.; Cronin, B.; Devine, A. L.; Dixon, R. N.; Nix, M. G. D. *Science* **2006**, *312*, 1637−1640.
(19) Dian, B. C.; Longarte, A.; Zwier, T. S. *J. Chem. Phys.* **2003**, *118*, 2696.
(20) Sobolewski, A. L.; Domcke, W.; Dedonder-Lardeux, C.; Jouvet, C. *Phys. Chem. Chem. Phys.* **2002**, *4*, 1093−1100.
(21) Kang, H.; Dedonder-Lardeux, C.; Jouvet, C.; Martrenchard, S.; Gregoire, G.; Desfrancois, C.; Schermann, J. P.; Barat, M.; Fayeton, J. A. *Phys. Chem. Chem. Phys.* **2004**, *6*, 2628−2632.
(22) Mercier, S. R.; Boyarkin, O. V.; Kamariotis, A.; Guglielmi, M.; Tavernelli, I.; Cascella, M.; Rothlisberger, U.; Rizzo, T. R. *J. Am. Chem. Soc.* **2006**, *128*, 16938−16943.
(23) Nolting, D.; Marian, C.; Weinkauf, R. *Phys. Chem. Chem. Phys.* **2004**, *6*, 2633−2640.
(24) Gregoire, G.; Jouvet, C.; Dedonder, C.; Sobolewski, A. L. *Chem. Phys.* **2006**, *324*, 398−404.
(25) Serrano-Andres, L.; Merchan, M. *J. Mol. Struct.-Theochem.* **2005**, *729*, 99−108.
(26) Kang, H.; Dedonder-Lardeux, C.; Jouvet, C.; Gregoire, G.; Desfrancois, C.; Schermann, J. P.; Barat, M.; Fayeton, J. A. *J. Phys. Chem. A* **2005**, *109*, 2417−2420.
(27) Kang, H.; Jouvet, C.; Dedonder-Lardeux, C.; Martrenchard, S.; Gregoire, G.; Desfrancois, C.; Schermann, J. P.; Barat, M.; Fayeton, J. A. *Phys. Chem. Chem. Phys.* **2005**, *7*, 394−398.
(28) Boyarkin, O. V.; Mercier, S. R.; Kamariotis, A.; Rizzo, T. R. *J. Am. Chem. Soc.* **2006**, *128*, 2816−2817.
(29) Talbot, F. O.; Tabarin, T.; Antoine, R.; Broyer, M.; Dugourd, P. *J. Chem. Phys.* **2005**, *122*, 074310.
(30) Gregoire, G.; Kang, H.; Dedonder-Lardeux, C.; Jouvet, C.; Desfrancois, C.; Onidas, D.; Lepere, V.; Fayeton, J. A. *Phys. Chem. Chem. Phys.* **2006**, *8*, 122−128.
(31) Tabarin, T.; Antoine, R.; Broyer, M.; Dugourd, P. *Rapid Commun. Mass Spectrom.* **2005**, *19*, 2883−2892.
(32) Gregoire, G.; Dedonder-Lardeux, C.; Jouvet, C.; Desfrancois, C.; Fayeton, J. A. *Phys. Chem. Chem. Phys.* **2007**, *9*, 78−82.
(33) Christiansen, O.; Koch, H.; Jorgensen, P. *Chem. Phys. Letters* **1995**, *243*, 409−418.

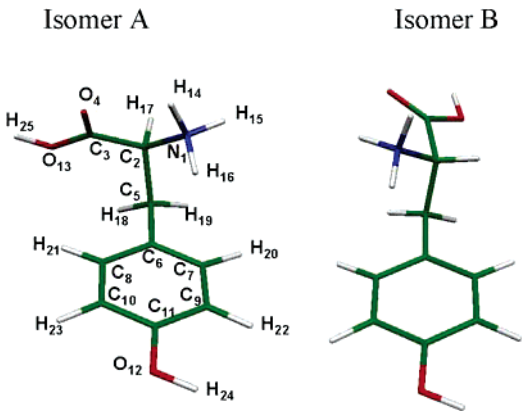

Figure 1. Atom labeling and ground state optimized structures of two low-lying isomers of protonated tyrosine (MP2). Isomer B is calculated 0.03 eV higher than isomer A.

The vertical and adiabatic energies along with the minimum energy path (MEP) of the first excited singlet states have been calculated at the CC2 level, making use of the recently implemented analytic CC2 gradients.[34]

These calculations were carried out with the TURBOMOLE (V.5-7-1) program suite,[35] making use of the resolution-of-the-identity (RI) approximation for the evaluation of the electron-repulsion integrals.[36] Calculations of the vertical excited-state energies have been performed using four different Gaussian basis sets in order to test basis set effect on the calculated quantities. The basis sets used range from the simple split-valence double-ζ Gaussian basis set with polarization functions on heavy atoms (def-SV(P)),[37] through the mixed def-SV(P) and the correlation-consistent Dunning-Hay valence double-ζ (cc-pVDZ),[38] up to the most extended basis set, aug-cc-pVDZ on all atoms. All these results, including vertical excitation energies and molecular structures, are reported in the Supporting Information.

As a compromise between the precision and the cost of calculations, all the results discussed in the paper, including ground state optimization at the MP2 level and excited-state properties and optimizations at the CC2 level, were obtained with the aid of the mixed basis set, def-SV-(P) on carbon and hydrogen atoms and aug-cc-pVDZ on nitrogen and oxygen atoms.

Results and Discussions

Protonated Tyrosine. Ground States Isomers. Two of the most stable conformers of protonated tyrosine were investigated. It should be noticed that the increase of strength of the proton bonding in protonated systems reduces the number of low-lying isomers as compared to the neutral one.[39,40] Atom labeling and two structures (isomer A and isomer B) are plotted in Figure 1. Their ground state optimized geometries are reported in Table 1. Their Cartesian coordinates are supplied in the Supporting Information. They differ from each other mainly by a $2\pi/3$ rotation of the amino acid moiety along the C_2-C_5 ($C_\alpha-C_\beta$) bond. For both isomers, the protonated amino group forms one proton bond to the carboxylic oxygen and one to the phenyl ring whereas one NH remains unbounded. In isomer A, which is more stable than isomer B by 0.03 eV at the MP2 level, both the NH_3 and the COOH groups lie above the phenyl ring, whereas in isomer B, the carboxylic acid moiety points away from the aromatic chromophore. As reported for protonated tryptophan,[24] structures with the protonated amino group pointing away from the chromophore are expected to lie much higher in energy and can be discarded.

Table 1. Optimized Gas-Phase Geometries for the Ground and First Excited-State of Isomers A and B of Protonated Tyrosine

	isomer A		isomer B	
	S_0[a]	S_1[b]	S_0[a]	S_1[b]
	Bonds (Å)			
N_1C_2	1.503	1.505	1.501	1.503
N_1H_{16}	1.045	1.075	1.041	1.076
N_1H_{15}	1.030	1.030	1.031	1.031
N_1H_{14}	1.040	1.043	1.038	1.043
C_2C_3	1.526	1.528	1.519	1.524
C_3O_4	1.217	1.226	1.218	1.226
C_3O_{13}	1.332	1.340	1.332	1.338
$O_{13}H_{25}$	0.984	0.987	0.984	0.987
C_2C_5	1.540	1.543	1.540	1.547
C_5C_6	1.507	1.499	1.506	1.498
C_6C_7	1.409	1.457	1.407	1.426
C_7C_9	1.402	1.441	1.398	1.418
C_9C_{11}	1.402	1.431	1.405	1.436
$C_{11}O_{12}$	1.359	1.350	1.360	1.351
$O_{12}H_{24}$	0.974	0.984	0.974	0.984
$C_{11}C_{10}$	1.406	1.429	1.404	1.424
$C_{10}C_8$	1.395	1.421	1.398	1.445
$C_8{}^cC_6$	1.411	1.422	1.410	1.453
	Dihedrals (deg)			
$C_6C_7C_9C_{11}$	−1	−14.7	1.2	4.2
$C_6C_8C_{10}C_{11}$	−0.8	−5.2	0.7	15.4
$C_7H_{20}C_9C_6$	2.7	18.3	1.5	0.1
$C_8H_{21}C_6C_{10}$	2	0.5	2.3	19.2

[a] MP2/SV(P) on C, H, and aug-cc-pVDZ on N, O calculations. [b] CC2/SV(P) on C, H, and aug-cc-pVDZ on N, O calculations.

Table 2. Vertical Excitation Energies (eV), Oscillator Strength, and Dipole Moment (in Debye) of Two Isomers of Protonated Tyrosine at the CC2 Level with the Mixed Basis Set, def-SV(P), on Carbon and Hydrogen Atoms and aug-cc-pVDZ on Nitrogen and Oxygen Atoms[a]

state	energy/eV	*f*	*μ*/debye	configuration
		Isomer A		
S_0	–	–	7.54	–
$\pi\pi^*/\pi 3p$	4.88	0.023	6.59	30%($\pi\pi_1^*$),29%($\pi 3p_{NH3}$)
$\pi\sigma^*$	5.73	0.037	9.32	77%($\pi\sigma_{NH3}^*$)
$\pi\pi^*$	5.87	0.233	4.95	21%($\pi\pi_2^*$),20%($\pi\pi_3^*$)
$\pi\pi_{CO}^*$	6.10	0.004	6.23	15%($n_{COOH}3p_{NH3}$),12%($\pi\pi_{CO}^*$)
		Isomer B		
S_0	(0.032)[b]	–	4.81	–
$\pi\pi^*/\pi 3p$	4.89	0.023	4.42	39%($\pi\pi_1^*$),32%($\pi 3p_{NH3}$)
$\pi 3p/\pi\sigma^*$	5.74	0.165	4.05	31%($\pi 3p_{NH3}$),23%($\pi\sigma_{NH3}^*$)
$\pi\sigma^*$	5.81	0.134	7.71	59%($\pi\sigma_{NH3}^*$)
$\pi\pi_{CO}^*$	6.10	0.025	5.34	16%($n_{COOH}3p_{NH3}$),12%($\pi\pi_{CO}^*$)

[a] Ground state energies (eV) are calculated at the MP2 level with the same basis set. [b] Ground state energy (eV) relative to the most stable isomer.

Vertical Excited-State Energies and Electronic Structures. Calculated vertical transitions of protonated tyrosine are reported in Table 2 and illustrated in Figure 2 (for more extended results see Supporting Information). The first four excited states are ordered in increasing energy along with their oscillator strengths and dipole moments. Within the accuracy of calculation, these isomers share several similarities. For both isomers, the S_1 state is noticeably separated from the higher excited states, with a

(34) Hattig, C. *J. Chem. Phys.* **2003**, *118*, 7751−7761.
(35) Ahlrichs, R.; Bar, M.; Haser, M.; Horn, H.; Kolmel, C. *Chem. Phys. Letters* **1989**, *162*, 165−169.
(36) Weigend, F.; Haser, M.; Patzelt, H.; Ahlrichs, R. *Chem. Phys. Letters* **1998**, *294*, 143−152.
(37) Schafer, A.; Horn, H.; Ahlrichs, R. *J. Chem. Phys.* **1992**, *97*, 2571−2577.
(38) Woon, D. E.; Dunning, T. H. *J. Chem. Phys.* **1993**, *98*, 1358−1371.
(39) Ramaekers, R.; Pajak, J.; Rospenk, M.; Maes, G. *Spectrochim. Acta, Part A* **2005**, *61*, 1347−1356.
(40) Grace, L. I.; Cohen, R.; Dunn, T. M.; Lubman, D. M.; de Vries, M. S. *J. Mol. Spectrosc.* **2002**, *215*, 204−219.

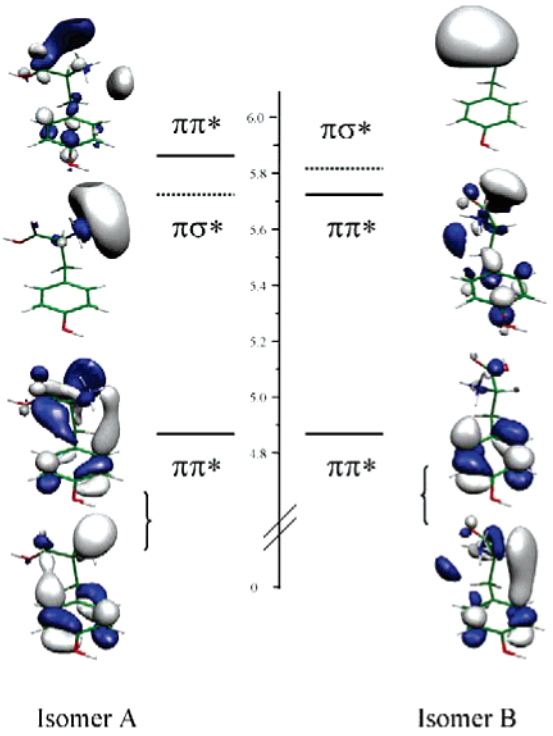

Figure 2. CC2 vertical excited-state energies along with the molecular orbital representation of the two isomers of protonated tyrosine. Full line, $\pi\pi^*$ state. Dotted line, $\pi\sigma^*$ state.

S_2/S_1 energy gap of about 0.8 eV at this level of theory. The electronic structure of the S_1 state is mainly of $\pi\pi_1^*$ character (L_b state in the Platt's nomenclature), corresponding to a $\pi_{HOMO-}\pi^*$ valence transition, with the latter containing a significant contribution from the 3p Rydberg orbital of the NH_3 group. The S_1 (L_b) oscillator strength is almost 1 order of magnitude lower than for the second $\pi\pi_2^*$ state (L_a state) that lies at much higher energy (roughly 1 eV), as for neutral tyrosine and phenol. The $\pi\pi_{CO}^*$ state is calculated even higher in energy with a very weak oscillator strength. Therefore, the two L_a and $\pi\pi_{CO}^*$ states are unlikely populated through 266 nm (4.66 eV) photon excitation. Note that the lowest unoccupied molecular orbital LUMO in both isomers has σ^* (3s Rydberg) character with electron density localized over the NH_3 group. The $\pi\sigma^*$ state is characterized by a larger dipole moment and similar oscillator strength as the L_b state.

The main difference between isomers A and B is related in the ordering of the higher excited states, with the $\pi\sigma^*$ state lower than the second $\pi\pi^*$ state in isomer A. In Figure 2 are plotted the relevant molecular orbitals involved in the electronic excitation to the lowest excited states of the two isomers. In general, the electronic nature of the excited states is difficult to assign because they are considerably mixed. Furthermore, the π^* orbitals are significantly delocalized over the whole system with some electron densities on carboxylic acid and amino groups.

Basis Set Effects. The effect of the basis set has been tested on both isomers, and the calculated vertical excitation energies are reported in tables TSI1 and TSI2 in the Supporting Information. The extension of the basis set up to aug-cc-pVDZ on all atoms lowers the excitation energies by about 0.2 eV for the lowest $\pi\pi^*$ state and by about 0.4 eV for the lowest $\pi\sigma^*$ state as compared to the basis set discussed above (Table 2).

The most important result of the calculated vertical excitation energies of protonated tyrosine is a large energy gap between the first $\pi\pi^*$ state and the $\pi\sigma^*$ state, which remains as large as 0.6 eV even for the most extended basis set used in the calculations. This relatively large energy gap was postulated in our previous work on the basis of simple energetic considerations.[27] The H atom dissociation energy of the N−H bond is calculated from asymptotic values of the proton affinity, the ionization energy of the amino acid and the ionization potential of hydrogen atom. If one assumes that the potential energy surface of the $\pi\sigma^*$ state along the dissociative N−H coordinate is not influenced by the nature of the aromatic chromophore, the vertical excitation energy of $\pi\sigma^*$ state at the ground state optimized geometry can thus be estimated for the different protonated amino acids, tryptophan and tyrosine, for instance. Accordingly, the $\pi\sigma^*/\pi\pi^*$ energy gap is expected to be 0.6 eV larger in tyrosine than in tryptophan, in fine agreement with the present result obtained with high level *ab initio* calculations.

Optimization of Excited-State Geometry. Optimization of the first excited-state has been performed at the CC2 level. The optimized geometries of the two isomers are reported in Table 1, and the Cartesian coordinates are supplied in the Supporting Information. The S_1 adiabatic energies are lowered by roughly the same amount for the two isomers, −0.25 and −0.26 eV in isomers A and B, respectively, which sets the calculated band origin at 4.63 eV for both isomers. The S_1 state optimization leads to a strong geometry rearrangement, in particular to substantial puckering of the aromatic ring that is indicated by the changes in the dihedral angles $C_6C_7C_9C_{11}$ and $C_6C_8C_{10}C_{11}$ of about 15° in isomers A and B, respectively (see Table 1). Besides, the hydrogen atoms bound to the C_7 (isomer A) and C_8 (isomer B) carbon atom significantly bend out of the aromatic ring by roughly 18°. Finally, the N_1H_{16} bond pointing toward the C_7/C_8 carbon atom of the phenyl ring elongates from 1.045/1.041 Å in S_0 to 1.075/1.076 Å in S_1 and the $N_1H_{16}-C_7/N_1H_{16}-C_8$ distances strongly shorten from about 2.4 Å to 1.985/1.978 Å in isomers A and B, respectively. The electronic structure of the S_1 state becomes a combination of $\pi\pi^*$ and $\pi\sigma^*$ configurations, the σ^* orbital being the 3s Rydberg type localized on the NH_3 group.

In construction of the reaction path for N−H bond cleavage of the protonated amino group, the coordinate-driven minimum-energy-path (MEP) approach was utilized, i.e., for a given N−H distance, all remaining intramolecular coordinates were optimized in the S_1 state. The MEP along the proton-transfer coordinate (NH distance) has been calculated for both isomers and exhibits a small barrier of 0.1 eV at a NH distance of 1.3 Å (Figure 3a). At a N_1-H_{16} distance of 1.8 Å (last point in Figure 3a), the N−H constraint is released and the S_1 state free optimization results in a proton transfer to the carbon C_7/C_8 of the phenyl ring in isomers A and B, respectively. Along the optimization process, the electronic nature of the excited molecular orbital changes gradually (Figure 3b) from a (almost) pure π^* orbital to a mixture of π^* with the σ^* orbital localized on the NH_3 group and eventually collapses again to a nearly pure π^* orbital of the aromatic ring.

It should be noticed that the S_1 state free optimization has not been completed because the S_1/S_0 energy gap vanishes and the near-degeneracy of the states causes convergence problems in the CC2 iteration cycle. In the proton transferred form of

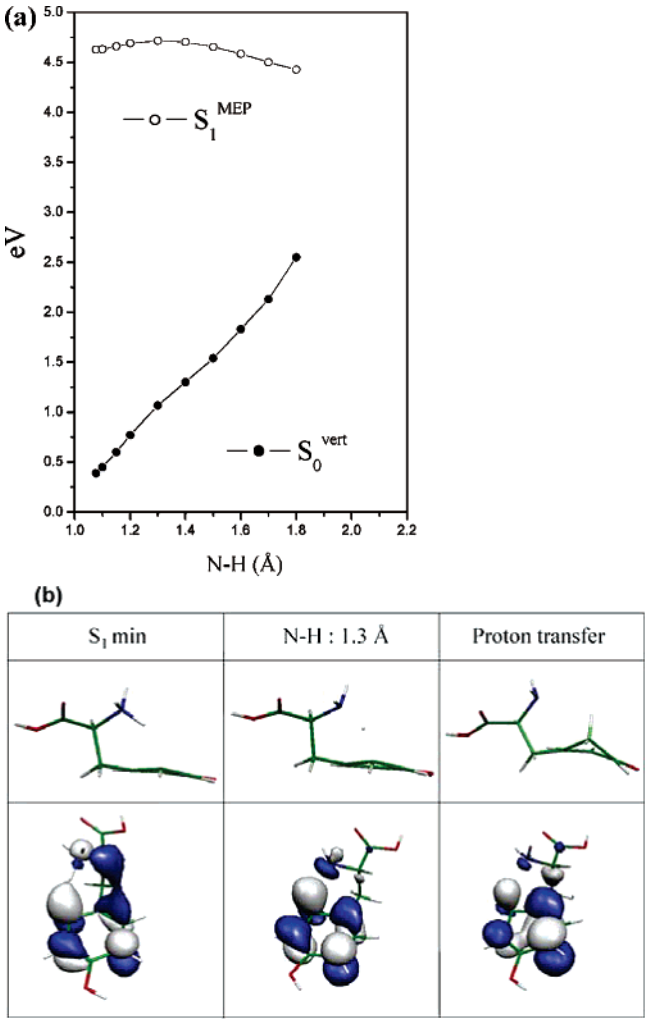

Figure 3. (a) S_1 Minimum Energy Path (MEP) for the proton-transfer reaction of protonated tyrosine (isomer B) along the N−H stretch to the phenyl ring. The zero energy refers to the ground state optimized structure (MP2). (b) Snapshots of the structure along the S_1 proton-transfer reaction of protonated tyrosine (isomer B) for given NH distances with their most relevant MO.

tyrosine reported in Figure 3b, the N_1-H_{16} distance increases to 2.6 Å and the dihedral angles $C_6C_7C_9C_{11}$ and $C_6C_8C_{10}C_{11}$ exceed 50 °. The adiabatic excited-state energy at this geometry is lowered by −0.66 eV from the optimized excited-state energy and the S_1/S_0 energy gap is reduced down to 0.35 eV. Starting from the geometry of the last converged point on the S_1 potential-energy surface, the MP2 geometry optimization of the ground state results in a back proton-transfer reaction to the NH_2 group. Due to the low-energy barrier and large stabilization energy of the proton-transfer reaction, UV excitation of protonated tyrosine is expected to lead to a fast and efficient internal conversion process.

The two other NH dissociation pathways have been investigated, the stretching of the NH-free bond and the NH bond pointing toward the carbonyl group. For the free NH bond, dissociation leads to the H-loss channel through a barrier of 0.8 eV (above the S1 vertical energy) for isomer A, and the barrier is higher (1 eV) for isomer B. For both isomers, the proton-transfer reaction to the carboxylic oxygen presents even higher barriers.

Comparison with Experiments. The calculations presented above can be compared with the recent UV photo-induced dissociation experiments carried out in our group using a femtosecond pump/probe scheme[27] and with the electronic spectroscopy performed in the group of T. Rizzo.[28] The electronic spectrum of cold $TyrH^+$ shows well resolved vibrational bands, with the origin band located at 4.35 eV. The O_0^0 band origin calculated in the present work, 4.63 eV with the medium size basis set is overestimated by 0.28 eV, which is within the expected accuracy of the CC2 method. Sharp vibrational progressions are observed in a quite narrow range up to 0.06 eV above the origin band, which clearly indicates that the excited state PES possesses a local minimum in the vicinity of the band origin, in agreement with our calculations. Furthermore, the electronic spectrum of room-temperature $TyrH^+$ has been recorded over a wider range in monitoring the intensity of ion fragment as a function of the laser wavelength and is therefore sensitive to the fragmentation efficiency. Although the spectrum is unresolved due to high internal energy of the ions, a second onset is observed roughly 0.1 eV above the origin that matches the calculated energy barrier of 0.1 eV found in this work for proton transfer to the phenyl moiety. This onset may be interpreted as an increase of the fragmentation yield above the barrier.

The excited-state lifetime of room-temperature $TyrH^+$ has been recorded after excitation at 266 nm (4.66 eV), i.e., 0.3 eV above the band origin.[27] The excess energy in the Franck Condon region is threefold higher than the calculated 0.1 eV barrier for proton transfer to the phenyl ring and should induce a very short excited-state lifetime. The relatively long lifetime of 22 ps measured for $TyrH^+$ may thus be related to a kinematic effect which involves a strong rearrangement of the molecule, formally a ring puckering, required for proton transfer to the ring. It should be noticed that, for protonated tryptamine, theory also predicts a similar barrier of about 0.1 eV in the first excited singlet state,[24] and the 250 fs excited-state lifetime measured is much shorter.[41] In the latter system, the excited-state lifetime is governed by the H-loss reaction involving the stretching of the NH bond of the amino group, without strong rearrangement of the whole system as in the former case. The measured difference between the excited-state lifetime of protonated tyrosine and tryptamine can thus be related to the mentioned above kinematic factor.

Protonated Tryptophan. Ground State Isomers. $TrpH^+$ is known to possess several isomers in aqueous solution where the side chain adopts various conformational states, the so-called rotamers.[1,8] $TrpH^+$ in the gas phase is also believed to exhibit such low-lying rotamers that mainly differ in the orientation of the amino-acid moiety above the indole chromophore by $2\pi/3$ rotation along of the $C_\alpha-C_\beta$ bond (see isomers A and C) and by π rotation along the $C_\gamma-C_\beta$ bond where C_γ is the carbon atom of the indole ring (see isomers B and D).[22] The lowest-energy protonation site of tryptophan is on the amino group, whereas protonation on the indolic nitrogen lies about 1 eV higher in energy.[42] Two rotamers with the protonated amino group away from the indole chromophore lie too high in energy (more than 0.35 eV above the global minimum) to be populated at 300 K. It should be emphasized that for each rotamer, a

(41) Kang, H.; Jouvet, C.; Dedonder-Lardeux, C.; Martrenchard, S.; Charriere, C.; Gregoire, G.; Desfrancois, C.; Schermann, J. P.; Barat, M.; Fayeton, J. A. *J. Chem. Phys.* **2005**, *122*, 084307.
(42) Lioe, H.; O'Hair, R. A. J.; Reid, G. E. *J. Am. Soc. Mass Spectrom.* **2004**, *15*, 65−76.

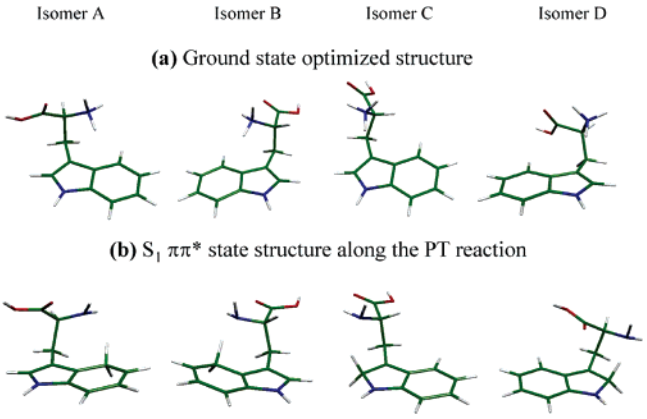

Figure 4. Four low-lying isomers of protonated tryptophan (a) S_0 ground state optimized structures (MP2). (b) Snapshots of the structures along the S_1 proton-transfer reaction.

Table 3. Vertical Excitation Energies (eV), Oscillator Strength, and Dipole Moment (in Debye) of the Four Compact Isomers of Protonated Tryptophan at the CC2 Level with the Mixed Basis Set, def-SV(P), on Carbon and Hydrogen Atoms and aug-cc-pVDZ on Nitrogen and Oxygen Atoms[a]

state	energy/ eV	f	μ/ debye	configuration
			Isomer A	
S_0	–	–	4.99	–
$\pi\pi^*$ (L_a/L_b)	4.90	0.031	4.75	23%($\pi_2\pi_9^*$), 21%($\pi_1\pi_3^*$)
$\pi\sigma^*$	5.04	0.045	2.77	32%($\pi_2\sigma_{NH3}^*$),16%($\pi_2\pi_3^*$)
$\pi\sigma^*/\pi\pi^*$	5.23	0.061	3.59	34%($\pi_2\sigma_{NH3}^*$), 30%($\pi_2\pi_3^*$)
$\pi\pi_{CO}^*/\pi\sigma^*$	5.69	0.030	7.96	29%($\pi_2\pi_{CO}^*$), 25%($\pi_1\sigma_{NH3}$)
			Isomer B	
S_0	(0.059)[b]	–	5.12	–
$\pi\pi^*$ (L_b)	4.92	0.025	4.83	35%($\pi_1\pi_3^*$), 20%($\pi_2\pi_9^*$)
$\pi\pi^*$ (L_a)	5.11	0.085	4.77	39%($\pi_2\pi_3^*$), 21%($\pi_2\sigma_{NH3}^*$)
$\pi\sigma^*$	5.32	0.033	5.84	51%($\pi_2\sigma_{NH3}^*$),19%($\pi_2\pi_3^*$)
π3p/$\pi\pi_{CO}^*$	5.71	0.021	10.30	35%($\pi_2$3p$_{NH3}$), 22%($\pi_2\pi_{CO}^*$)
Isomer C				
S_0	(0.08)[b]	–	5.14	–
$\pi\pi^*$ (L_b)	4.92	0.032	4.62	27%($\pi_1\pi_3^*$), 19%($\pi_1$3p$_{NH3}$)
$\pi\sigma^*$	5.08	0.038	3.72	58%($\pi_2\sigma_{NH3}^*$)
$\pi\pi^*$ (L_a)	5.33	0.12	2.63	32%($\pi_2\pi_3^*$), 18%($\pi_2\sigma_{NH3}^*$)
$\pi\sigma^*$	5.71	0.018	8.07	72%($\pi_1\sigma_{NH3}^*$)
Isomer D				
S_0	(0.087)[b]	–	8.06	–
$\pi\pi^*$ (L_b)	4.88	0.038	7.06	20%($\pi_1\pi_3^*$), 20%($\pi_1$3π_{NH3})
$\pi\sigma^*$	5.03	0.031	5.84	68%($\pi_2\sigma_{NH3}^*$)
π3p/$\pi\pi^*$(L_a)	5.31	0.09	5.77	34%($\pi_2$3p$_{NH3}$), 18%($\pi_2\pi_3^*$)
π3p	5.53	0.09	7.51	19%($\pi_2$3p$_{NH3}$), 16%($\pi_2$3p$_{NH3}$)

[a] Ground state energies (eV) are calculated at the MP2 level with the same basis set. [b] Ground state energy (eV) relative to the most stable isomer.

rotation of π of the carboxyl group along the $C_\alpha-C_{OOH}$ bond leads to an equilibrium structure that lies about 0.13 eV higher in energy with a barrier to the rotation calculated at 0.4 eV. These isomers can thus be discarded. The structures of the four lowest-energy rotamers are shown in Figure 4a and their respective energies (calculated at the MP2 level) are reported in Table 3.

Vertical Excited-State Energies and Electronic Structures. Because the system has no symmetry, the labeling of the states is quite difficult. The molecular orbitals are more or less localized (indole ring, amino group, carbonyl group), but the excited-state wavefunctions are combination of several electronic configurations. Ideally, the electronic structure of the excited-state can be defined as follows:

- the L_b state, characterized by the excitation from the π_{HOMO-1} to a π^* orbital, both localized on the indole ring, noted $\pi_1 p_j^*$ ($j \geq 3$).

- the L_a state, characterized by the excitation from the π_{HOMO} orbital to a π^* orbital, both localized on the indole ring, noted $\pi_2 p_j^*$ ($j \geq 3$).

- the $\pi\sigma^*$ state, characterized by the excitation from the π_i orbital, (i being 1 or 2, i.e., the π_{HOMO-1} or π_{HOMO} orbital localized on the indole ring) toward the σ^* Rydberg-type orbital localized on the NH_3 group, noted $\pi_i\sigma_{NH3}^*$.

- the π3p state, characterized by the excitation from the π_i orbital (localized on the indole ring) toward a $3p_{NH3}$ localized on the NH_3 group, noted $\pi_i 3p_{NH3}$.

- the $\pi\pi_{CO}^*$ state, corresponding to the excitation from the π_{HOMO} to a π^* orbital mainly localized on the carboxylic acid group, noted $\pi_2\pi_{CO}^*$

Basis Set Effect. The basis set effect has been tested on the two lowest energy isomers A and B and the calculated vertical energies are reported in Tables TSI3 and TSI4 of the Supporting Information. The results obtained for $TrpH^+$ are much more complicated than for $TyrH^+$ due to the dense manifold of low-lying excited singlet states of different orbital nature. As the number of basis functions increases, the vertical excitation energies decrease roughly by 0.1−0.3 eV and a pronounced mixing between the excited states occurs, especially the $\pi\pi^*$ and the $\pi\sigma^*$ states are getting highly mixed. Therefore, the labeling of the state is quite tenuous and depends on the basis set used, but the overall picture remains qualitatively similar. This mixing is reflected by the rather similar oscillator strengths borne by the different excited-state as can be seen in Table 3. This is in straight contrast with protonated tyrosine where the first excited-state still remains of $\pi\pi^*$ character without strong mixing with the σ^* orbital.

As can be seen from Table 3 and in Figure 5, the four isomers share several similarities. The L_b and L_a states are always within the three lowest excited states, the L_b state having a vertical energy always lower than the L_a although they are strongly mixed with each other (see isomer A) and with the $\pi\sigma^*$ and π3p states. The $\pi\pi_{CO}^*$ states lies always much higher than the $\pi\pi^*$ state. Finally depending on the isomer, the $\pi\sigma^*$ state is located either below or above the L_a state. In isomers C and D for instance, the first $\pi\sigma^*$ state that corresponds to a π_2 to σ_{NH3}^* transition lies significantly below the L_a state by about 0.25 eV. One will see below that geometry optimization of the S_2 $\pi\sigma^*$ state for these two specific isomers leads to an excited-state hydrogen transfer to the carboxylic acid group.

Optimization of Excited-State Geometry. Geometry optimizations have been performed for the four isomers of $TrpH^+$ in their first and second excited singlet states. In the case of S_2 optimization, the calculation is stopped when the S_1/S_2 crossing point is reached. The geometry obtained at this last point is used as a starting point for an optimization on the S_1 surface, which goes on until the convergence criteria are fulfilled or until a second crossing with the electronic ground state is reached.

Some general features can be drawn from these calculations. First, independently of the isomer, optimization of the S_1 $\pi\pi^*$ excited singlet state results in a barrierless proton transfer from the NH_3^+ group to the indole chromophore (Figure 4b). This is in contrast with protonated tyrosine, which exhibits a barrier of about 0.1 eV for this reaction. Second, optimization started

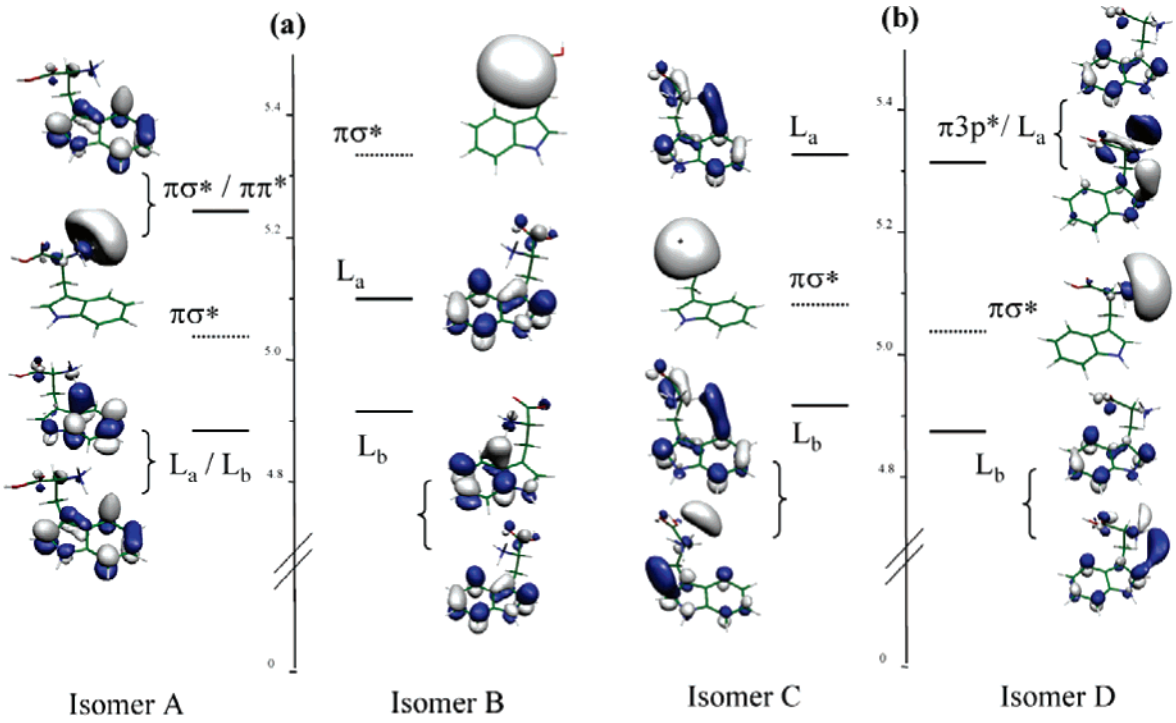

Figure 5. CC2 vertical excited-state energies along with the molecular orbital decomposition of the 4 low-lying isomers of protonated tryptophan. Full line, L_b and L_a states; dotted line, $\pi\sigma^*$ state; (a) isomer A and isomer B; (b) isomer C and isomer D.

on the S_2 excited singlet state, and carried on the S_1 state PES after the S_1/S_2 crossing, leads to different reactive channels depending on the isomer. In isomers A and B, where the $\pi\sigma^*$ state lies above the L_a state, the same proton-transfer reaction to the indole chromophore is observed as for optimization of the S_1 state. However, for isomers C and D, where the S_2 $\pi\sigma^*$ state is below the S_3 L_a state, a spontaneous hydrogen transfer reaction to the carboxylic oxygen occurs.

In the following, the course of the different optimizations leading to the proton transfer and to the hydrogen atom transfer reactions is discussed in more details. It should be noted that because all the optimizations lead to exothermic reactions without barriers, no stationary points have been obtained.

Proton-Transfer Reaction. Proton transfer to the indole ring involves deformation of the ring around the proton accepting carbon atom (C4 for isomer A and B or C2 for isomers C and D following the atom labeling of the indole ring moiety as reported in ref 42). This deformation includes the CH out-of-plane bending (20°) and a ring puckering (10−15°) as observed in the case of protonated Tyr. When the optimized state corresponds to the L_b state as in isomers B, C, and D, the electronic structure of the optimized S_1 evolves quickly along the proton-transfer reaction coordinate and is characterized by a $\pi_{HOMO}-\pi^*$ electronic configuration. As the NH−C bond distance decreases, the π^* orbital localized on the indole moiety gets some electronic density outward the indole ring and no more changes are observed in the course of the reaction. Starting from the geometry of the last converged point on the S_1 potential-energy surface, MP2 optimization of the ground state leads to a proton-transfer reaction back to the NH_2 group, as calculated for Tyrosine.

The proton-transfer reaction involves ring puckering and CH bending mode. We have performed S_1 optimization under geometry constraints, including planarity of the ring and CH bending mode. Interestingly, it leads to a stable structure with stabilization energy of −0.17 eV with respect to the vertical transition energy (calculated for isomer B) where the S_1 state keeps its L_b electronic configuration, the L_a state being located 0.34 eV above. When the geometry constraints are released, the proton-transfer reaction is observed.

Hydrogen Atom Transfer to the Carboxylic Acid Oxygen (Isomers C and D). Optimization of the $\pi\sigma^*$ state, which is the second excited-state in isomers C and D leads to a spontaneous (barrierless) hydrogen transfer reaction to the carboxylic oxygen. In these two isomers, this state corresponds to the first $\pi_{HOMO}-\sigma_{NH3}^*$ transition and lies below the L_a state ($\pi_{HOMO}-\pi^*$ transition localized on the indole ring). S_2 structure optimization is first initiated until the S_2/S_1intersection is reached, and needs to be restarted on the S_1 excited-state surface. At the S_2/S_1 intersection, there is a slight breaking of the planar symmetry of both the acidic group and the smallest one on the indole ring (the indole ring is tilted by 3° from the plane defined by the benzene ring). It however induces significant stabilization energy of −0.17 and −0.24 eV as compared to the vertical excitation energies for isomers C and D, respectively. Thus, as suggested by the results reported in Table 3, very small geometry differences strongly affect the ordering of the electronic states and have a strong impact on the result of the excited-state optimization.

For Isomer D (Figure 6), when the S_2/S_1 intersection is reached, the electronic structure of the S_1 state is a combination of a σ^* type orbital on the amino group and a delocalized π^* orbital on the indole ring with some electronic density on the carboxylic group. When the excited-state optimization goes on, this latter orbital collapses to a π^* orbital located on the carboxylic group, which corresponds to an electron transfer from the indole chromophore to the carboxylic acid group that induces the proton transfer from the amino group to the carboxylic

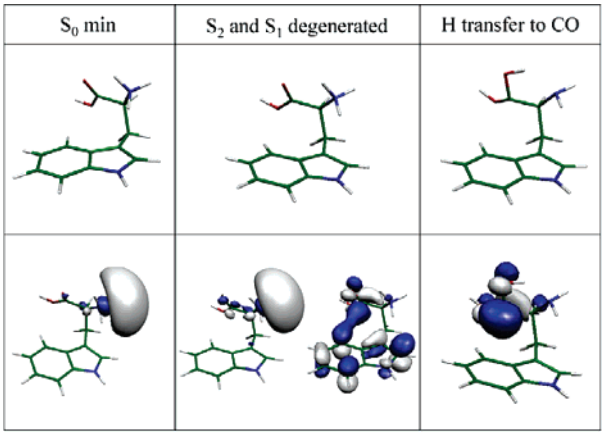

Figure 6. Snapshots of the structure along the H transfer reaction to the carboxyl oxygen of protonated tryptophan (Isomer D) with their most relevant molecular orbitals.

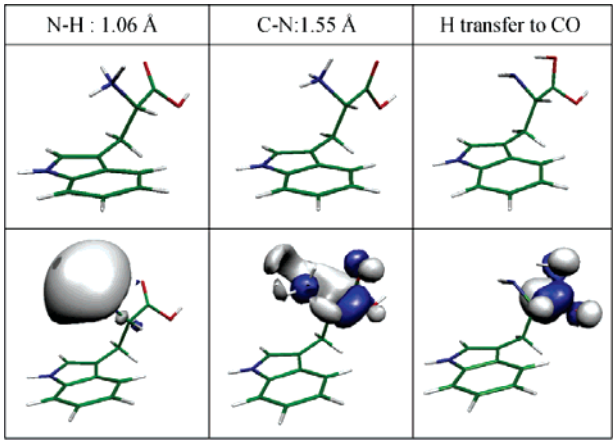

Figure 7. Snapshots of the structure along the H transfer reaction to the carboxyl oxygen of protonated tryptophan (Isomer C) with their most relevant molecular orbitals. See text for details.

oxygen. This hydrogen atom transfer reaction can thus be viewed as an electron-driven proton-transfer process with the two events decoupled in time and space.

In the case of isomer C, the optimization path is even more complex. A direct electron transfer from the indole moiety to the carboxylic acid group is unlikely because this group is not interacting with the chromophore (Figure 7). During the excited-state optimization after the S_2/S_1 crossing is reached, the N−H bond first elongates from 1.04 to 1.06 Å, the C−N bond next stretches from 1.50 to 1.55 Å. At this point, the electronic structure of the excited-state is mainly determined by a delocalized orbital on both the amino and the acidic groups, which collapses into a localized orbital on the carboxylic acid group after the H atom transfer has occurred.

The H atom transfer reaction leads to a biradical ion with a positive charge on the indole ring and an unpaired electron on the aliphatic carbon. Such electronic configuration may induce the $C_\alpha-C_\beta$ bond rupture directly in the excited-state that leads to the detection of Trp side chain *m*/*z* 130 fragment. Further calculations will be necessary to investigate the fragmentation channels of this radical species.

Hydrogen Atom Loss Reaction. None of the excited-state optimization leads to the hydrogen atom loss reaction, which is observed experimentally, at the opposite to the protonated tryptamine case where the H atom loss is established experimentally and theoretically. On the other hand, the proton-transfer reaction has not been evidenced in protonated tryptamine, even when stretching the N−H bond directed toward the indole ring. Excited-state optimization of protonated tryptamine leads to the H atom loss reaction through a small barrier along the N−H stretch coordinate (0.1 eV) or to the NH_3 loss process through a higher barrier of 0.3 eV.[24] Therefore, an energy barrier to H atom loss is also conjectured in the case of protonated tryptophan.

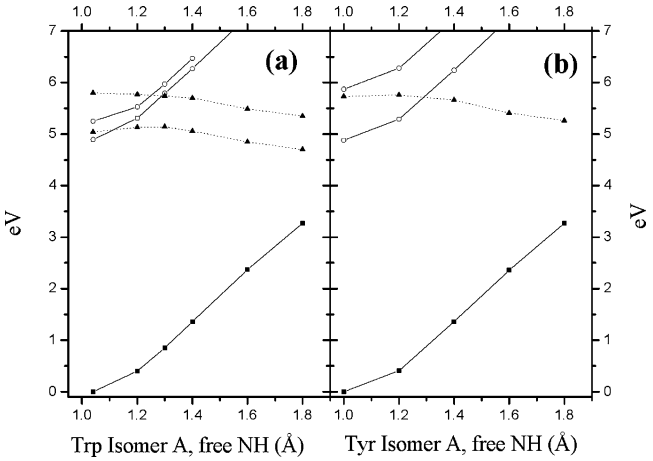

Figure 8. CC2 vertical excited-state energies along the free N−H stretch. ■, S_0 ground state; ○, $\pi\pi^*$ state; ▲, $\pi\sigma^*$ state; (a) isomer A of protonated tryptophan. The barrier for H atom loss reaction is 0.2 eV; (b) isomer A of protonated tyrosine. The barrier for H atom loss reaction is 0.8 eV.

We have performed several vertical excited-state calculations on different isomers for which the free N−H bond is stretched gradually while keeping the rest of the intramolecular coordinates at their ground-state optimized values. The results are reported in Figure 8a for isomer A. Under these geometrical constraints, the H atom loss reaction occurs through a small barrier of about 0.2 eV at a N−H bond distance of 1.3 Å. Therefore, even if this channel is not favored by the optimization procedure due to the presence of a small barrier, it may be favored through dynamics because H loss is a single coordinate process that involves the motion of a light atom, whereas proton transfer requires a more complex mechanism with amino chain and indole ring deformation and may occur on a longer time scale. It is noteworthy that the same H loss reaction exhibits a much higher barrier in the case of protonated tyrosine (Figure 8b), of the order of 0.8 eV at a N−H distance of 1.3 Å. This agrees well with the absence of the H loss channel in protonated tyrosine excited at 266 nm.

Comparison with Experiments. The present calculations have to be related with the spectroscopic and dynamics studies performed on protonated tryptophan by several groups.[26,28,29] All the electronic spectra of protonated tryptophan are broad without sharp features, even at the very low temperature achieved in T. Rizzo experiment.[28] This has been rationalized in terms of short excited-state lifetime, even at the band origin. Our present calculations show that the first $\pi\pi^*$ excited singlet state reacts without barrier via proton transfer, which agrees quite well with these spectroscopic results.

By scanning the excitation wavelength from the band origin to higher energies, P. Dugourd et al.[29] have shown that the branching ratio between the different ionic fragments changes drastically. Near the band origin (285 nm, 4.35 eV), the main

fragmentation channels are those usually observed in collision induced dissociation experiments and are thus related to an internal conversion process following UV excitation. A smooth increase of the tryptophan radical cation yield (issued from the H loss) is observed around 270 nm (4.60 eV) that extends up to 240 nm where its specific secondary fragment *m*/*z* 130 sharply increases. Near the band origin, the proton-transfer reaction leading to internal conversion is predominant while at higher energy, the H atom loss reaction occurs above a barrier of about 0.25 eV in agreement with our calculations.

Competition between these two reactive processes has been evidenced in our femtosecond pump/probe experiment.[26] Protonated tryptophan exhibits an ultrafast decay with two time constants of 400 fs and 15 ps. Although the short lifetime component has been ascribed to the dynamics on the $\pi\sigma^*$ state surface along the free NH stretch coordinate as for protonated tryptamine, the interpretation of the 15 ps time constant was unclear. Because the pump photon excites the molecule at 266 nm, both proton transfer and H transfer reactions are allowed and both IC-type and radical cation-type fragments are detected. With the help of the excited-state calculations reported here and by comparing with protonated tyrosine, we assign the 15 ps time constant of protonated tryptophan to the dynamics on the $\pi\pi^*$ state that decays through proton transfer to the indole ring.

Conclusions

Vertical excited-state energies and excited-state optimizations at the CC2 level have been performed for low-lying isomers of protonated tyrosine and tryptophan and are compared to recent experimental results. The longer excited-state lifetime recorded for tyrosine is explained by the larger energy gap between the locally excited $\pi\pi^*$ state and the dissociative $\pi\sigma^*$ state, which confirms the initially proposed model based on simple energetic consideration. For both species, the $\pi\pi^*$ state undergoes a proton-transfer reaction from the amino group to the aromatic chromophore, that provides an efficient and fast pathway for internal conversion. This reaction occurs without barrier in the case of protonated tryptophan or with a small barrier of 0.1 eV in protonated tyrosine. This reaction involves changes in several internal coordinates with a ring puckering and a CCH out-of-plane bending. Although this reaction exhibits a small or no barrier, the large deformation of the molecule implies a longer excited-state lifetime than direct bond dissociation in the excited state (as for protonated tryptamine). In protonated tryptophan, the manifold of excited states in the Franck Condon region allows to open other reaction channels, such as a barrierless H atom transfer to the carboxylic acid oxygen or the H atom loss process through a small barrier of roughly 0.2 eV. These two reaction paths can compete with the barrierless proton-transfer reaction because only one N−H stretching coordinate is involved.

Although the role of the $\pi\sigma^*$ state in isolated protonated aromatic amino acids and peptides with an ammonium group in the vicinity of the aromatic chromophore is now clearly evidenced, one can wonder what will be the solvation effect on the excited-state properties. Protein folding can be studied by changes in the fluorescence intensities or emission spectra as the tryptophan residue becomes more or less expose to water environment. The origin of multiexponential decays in single-tryptophan proteins is thought to be related to the existence of such multiple protein conformations. As T. Rizzo reported very recently,[22] $TrpH^+$ complexed with two water molecules exhibits a vibrationally resolved excitation spectrum, emphasizing an increase of the excited-state lifetime of these hydrated species. We are presently working on a new hydrated electrospray ion source to record the excited-state lifetime of mass-selected $TrpH^+-(H_2O)_n$ clusters by means of pump/probe photofragmentation spectroscopy.

Acknowledgment. We are grateful to Pr. T. R. Rizzo for providing us his experimental and theoretical results prior to publication.

Supporting Information Available: Vertical excited-state energies of protonated tyrosine and tryptophan using different basis sets along with the Cartesian coordinates of ground and excited-state optimized structures. This material is available free of charge via the Internet at http://pubs.acs.org.

JA069050F